Reviewed research article

Continuous monitoring of ice dynamics in Iceland with Sentinel-1 satellite radar images

Jan Wuite[1], Ludivine Libert[1], Thomas Nagler[1] and Tómas Jóhannesson[2]
[1]*ENVEO Environmental Earth Observation IT GmbH, Fürstenweg 176, A-6020 Innsbruck, Austria*
[2]*Icelandic Meteorological Office (IMO), Bústaðavegur 7–9, IS-105 Reykjavík, Iceland*
Corresponding author jan.wuite@enveo.at; https://doi.org/10.33799/jokull2021.72.001

Abstract — *In recent years, satellite remote sensing has revolutionized observations of glacier dynamics enabling for the first time the generation of detailed ice-velocity fields at regular intervals for Icelandic glaciers. We generated dense time series of ice-velocity fields from 2014 to 2020 exploiting the continuous acquisition of Sentinel-1 SAR using the offset-tracking technique. The fastest ice flow, with velocities up to 400–800 metres per year, is observed in the middle and lower part of the main outlet glaciers of the ice caps that span a large elevation range in the areas of high precipitation in the South and Southeast of Iceland. Several outlet glaciers of Vatnajökull, such as Skeiðarárjökull and Breiðamerkurjökull, draining towards the South and Southeast, show high-ice-speed channels with pronounced shearing zones where the ice speed increases by an order of magnitude within a distance of only a few ice thicknesses. Velocities on the order of a few tens of metres per year, and up to 50–100 metres per year, are observed on the large surge-type outlet glaciers of N- and W-Vatnajökull and generally on glaciers in the central Icelandic highland and in the northern and western part of the country. Slow-moving ice is observed along the main ice divides and near the glacier margins. The velocity data set is affected by gaps due to decorrelation, particularly during summer, because of temporal variations in the radar-image texture. The ice-velocity fields derived in this study from Sentinel-1 data agree well with other data sets, although these are affected by a larger number of outliers and data gaps, particularly in the accumulation areas. The generated velocity time series can be used for monitoring long-term dynamic trends, seasonal variations and for studying glaciological events such as surges or jökulhlaups.*

INTRODUCTION

Remote sensing of ice flow, in combination with advanced processing and analysis for inversion of dynamic flow fields at depth within glaciers, has created new possibilities for studies of ice dynamics (Rignot *et al.*, 2002; Morlighem *et al.*, 2010; Nagler *et al.*, 2015, 2016; Gardner *et al.*, 2018). It is now possible to operationally monitor surface ice-velocity fields for entire glaciers globally based on regular acquisition of radar and optical satellite images (Mouginot *et al.*, 2017, 2019; Gardner *et al.*, 2021; ENVEO, 2021; Friedl *et al.*, 2021). These measurements allow for the analysis of glaciological processes that are important for projecting future response of glaciers to climate change, for studying glaciological hazards and interpreting poorly understood glaciological phenomena that await scientific explanation. Icelandic glaciers offer unique conditions to assess the potential of this new technology because of the availability of data from earlier studies, ease of access for new field studies and a high frequency of outstanding glaciological events (surges, jökulhlaups, subglacial volcanic eruptions) for scientific studies.

The first quantitative measurements of ice-flow velocities in Iceland with geodetic instruments were made on the Hoffellsjökull outlet glacier in southeastern Vatnajökull during the Swedish–Icelandic investigations of 1936 to 1938 (Þórarinsson, 1939), and on the Morsárjökull outlet glacier of Öræfajökull in southern Vatnajökull by Jack Ives and his colleagues from the University of Nottingham in the early 1950s (Ives and King, 1954, 1955). The measurements on Hoffellsjökull showed the transverse velocity profile across the glacier at ca. 450 m a.s.l., 7 km upstream of the snout, with a maximum velocity ca. $2\,\mathrm{m\,d^{-1}}$, and a longitudinal profile with lower velocities near the snout in the eastern branch of the glacier. Ives *et al.* measured flow velocities in the range of 0.2–$0.5\,\mathrm{m\,d^{-1}}$ in the ablation area of Morsárjökull and established that ogives on the glacier surface were annual phenomena which could be used to estimate the long-term velocity of the ice flow. They also noticed that the ice velocity varied with time during the summer by more than a factor of two. Interestingly, observations of the geometry of ogives on the Hrútárjökull outlet glacier on the other side of Öræfajökull in 1793 and 1794, one and a half centuries earlier by Sveinn Pálsson (2004, written in 1795), were most likely the first observations of the movement of glaciers in Iceland. Sveinn Pálsson concluded from observations of the geometry of the ogives that the glacier "had flowed down in a semi-melted or thick and viscous state" but he did not quantify the rate of movement. Pálsson's deduction about slow viscous movement of glacier ice was made at the time when the first glaciologists in Europe reached the same conclusion based on observations in the Alps (see the editors' introduction and endnotes in Pálsson, 2004). After Pálsson's qualitative observations in the 18^{th} century, the only observations of ice flow in the Icelandic glaciers, until Þórarinsson measurements in the late 1930s, were made by Otto Torell (1857) on Svínafellsjökull, an outlet glacier in Öræfajökull. Torell measured a flow velocity of ca. $0.25\,\mathrm{m\,d^{-1}}$ about 1.5 km upstream of the terminus with rudimentary equipment (Þórarinsson, 1939).

Regular stake measurements of ice-flow velocity in Iceland did not start until the early 1990s with the establishment of mass-balance programmes on Hofsjökull, Vatnajökull and Langjökull ice caps (Björnsson and Pálsson, 2008; Björnsson, 2009/2017; Aðalgeirsdóttir *et al.*, 2020), which provided seasonal velocities at a few dozen points on each ice cap. These were followed by several interferometric radar and offset-tracking studies of ice-flow velocity and uplift over limited areas or single ice caps over short time periods (e.g. Björnsson *et al.*, 2001; Guðmundsson *et al.*, 2002; Fischer *et al.*, 2003; Berthier *et al.*, 2006; Magnússon, 2007, 2008, 2010, 2011; Nagler *et al.*, 2012; Minchew *et al.*, 2015, 2016). In recent years, GPS stations have been continuously operated at several locations on glaciers in Iceland over extended periods of time, yielding high temporal resolution ice-flow velocities, for example for studying glacier dynamics and jökulhlaups (e.g. Magnússon *et al.*, 2011; Einarsson *et al.*, 2016). These previous measurements have shown the overall magnitude and given some information on the spatial distribution and variations with time of ice-flow velocity on the Icelandic glaciers. They have shed light on many glaciological events at several locations, but data coverage has been insufficient to show the overall spatial pattern of ice flow or monitor seasonal ice-flow variations or variations with time during events such as surges.

The ice flow of glaciers shows variations on a range of spatial and temporal scales. Spatially contiguous ice-velocity fields from space- and airborne remote-sensing data (e.g. Nagler *et al.*, 2015; Mouginot *et al.*, 2017, 2019) show that the ice flow tends to be channelled into narrow corridors of high velocity surrounded by areas with substantially lower ice-flow velocities. This pattern is particularly conspicuous on the large ice sheets of Antarctica and Greenland (Nagler *et al.*, 2015; Mouginot *et al.*, 2017, 2019), where these ice-flow channels are called ice streams, but such spatial patterns have also been observed on the ice caps of Iceland (Magnússon *et al.*, 2007; Minchew *et al.*, 2015) and other smaller glaciers and ice caps (e.g. Strozzi *et al.*, 2017). Changes in the mass discharge of the ice streams of Antarctica and Greenland are thought to be important with regard to the contribution of the ice sheets to global sea-level rise, in particular for the currently ongoing dramatic increase in the rate of ice discharge from many areas in Antarctica and Greenland (Mouginot *et al.*, 2018; Rignot *et al.*, 2019). Therefore, studying the short- and long-term variation of the ice-flow pattern and velocity of

Icelandic glaciers and ice caps is an important contribution to assessing the effects of the ongoing warming in the Arctic region.

In this paper, we present and analyse time series of ice-velocity fields from offset-tracking applied to Copernicus Sentinel-1A/B radar images of the Icelandic glaciers from 2014 to 2020. We compare the products with long-term velocity fields from the global RETREAT ice-velocity data set (Friedl *et al.*, 2021) and the NASA MEaSUREs ITS_LIVE project (Gardner *et al.*, 2021). The paper describes the Sentinel-1 data availability and the operational ice-velocity processing, providing background for use of the public domain ice-velocity data in other studies. Validation of the obtained ice velocities with available point measurements of mass-balance stakes and data from continuous GPS-stations is ongoing and will be described in subsequent papers.

DATA AND METHODS

Sentinel-1 data

The Copernicus Sentinel-1 (S-1) mission is a constellation of C-band Synthetic Aperture Radar (SAR) satellites operated by ESA and currently consisting of Sentinel-1A (S-1A) and Sentinel-1B (S-1B), launched in April 2014 and 2016 respectively. S-1 covers the European domain systematically every 6 to 12 days. The launch of Sentinel-1C is scheduled for the end of 2022/early 2023 and will guarantee the continuity of the ongoing acquisitions in coming years. The open-data policy of Copernicus provides S-1 data free of charge through the Copernicus Open Access Hub (SciHub) and various mirror sites.

Over land areas, S-1 operates mainly in Interferometric Wide (IW) swath mode, which exploits the TOPS (Terrain Observation by Progressive Scans) technique and provides a large swath width of 250 km at a nominal ground resolution of 5×20 m for single-look data, offering enhanced image performance compared with the conventional ScanSAR mode (De Zan and Monti Guarnieri, 2006). The ice-velocity products presented in this paper are generated using Level-1 IW Single Look Complex (SLC) images. Detailed technical information about the S-1 radar data is given by Yagüe-Martínez *et al.* (2016).

S-1A has provided continuous coverage for Iceland since October 2014 with a 12-day repeat-pass period. With the launch of S-1B in April 2016, the repeat-pass period was reduced to 6 days. Data for Iceland are acquired in both ascending and descending directions, providing also opportunities for interferometric applications or the retrieval of the full 3D velocity vector applying the in-coherent offset tracking technique (Nagler *et al.*, 2012), although not yet implemented in the automated processing line. Figure 1 shows the continuous 6-day and 12-day S-1 repeat tracks covering Iceland according to the acquisition in 2020. The histogram shows the available number of image pairs for each mission year indicating how coverage has improved over time, particularly after S-1B became operational.

ENVEO Sentinel-1 ice velocity

The ice-velocity products presented and evaluated in the next sections are generated by applying offset-tracking to S-1 data (Nagler *et al.*, 2015). Offset-tracking is a technique that aims at measuring local registration offsets with image chip correlation. In the context of ice monitoring, the offsets correspond to surface features such as crevasses, rifts or edges moving with the ice flow, and those features can be tracked using SAR amplitude images as template (Gray *et al.*, 2001; Strozzi *et al.*, 2002; Joughin, 2002).

The processing line developed by ENVEO for ice-velocity retrieval with S-1 data is depicted in Figure 2. For each pair, the processing starts with a geometric coregistration of the bursts based on the precise orbit annotations and an external digital elevation model (DEM) (lidar DEMs from 2008–2013 for the glaciers and adjacent proglacial areas (Jóhannesson *et al.*, 2013) and a countrywide 25x25 m composite DEM derived by the IMO and ÍSOR from various sources for ice-free areas, both resampled to 100x100 m). After the coregistration, the offset-tracking module is run at the burst level. The offset-tracking module consists of (1) oversampling the SLC bursts by a factor 2 in both the azimuth and slant range dimensions, (2) generating the amplitude images from the over-sampled SLCs, and (3) calculating the 2D normalized cross-correlation of the amplitude chips, finding the azimuth–slant-range sub-pixel position of the cross-

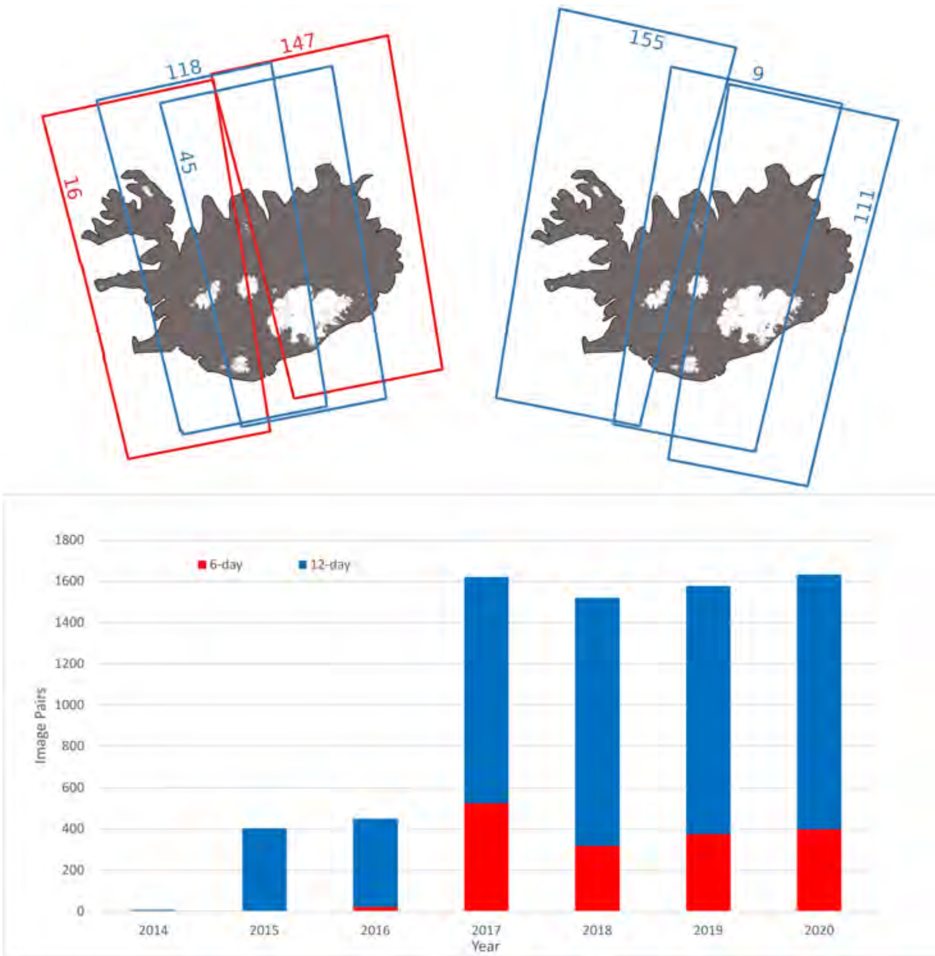

Figure 1: Continuous 6-day (red) and 12-day (blue) Sentinel-1 IW swath mode repeat acquisition in Iceland in 2020 (left: ascending; right: descending; track number indicated) and histogram showing the number of image product pairs for each mission year. Glacier extent in ∼2000 from Sigurðsson *et al.* (2017) are shown in white. – *Fótspor og fjöldi Sentinel-1 radarmyndpara með 6 og 12 daga millibili fyrir Ísland á árinu 2020 og árlegur fjöldi myndpara með 6 og 12 daga millibili á tímabilinu 2014–2020.*

correlation peak which corresponds to the measured 2D-offset, and estimating the height of the correlation peak. Measurements with low correlation peaks are dismissed and the estimated offsets are directly converted to azimuth and slant-range velocities. The offset-tracking module is run on each pair of bursts separately, thus yielding a stack of 2D-velocity burst images as output.

The 2D-velocity image at the track-scale is obtained by stitching the burst images together during the debursting process. The so-called debursted image is calculated in radar geometry and its extent in the along-track and across-track directions is defined respectively by the slant-range and azimuth time minimum and maximum values within the stack of burst images. The pixel spacing of the debursted image is determined by the slant-range and azimuth sampling rates, which are constant parameters for all S-1 bursts in IW mode. The debursted image is obtained by resampling successively each burst image on the

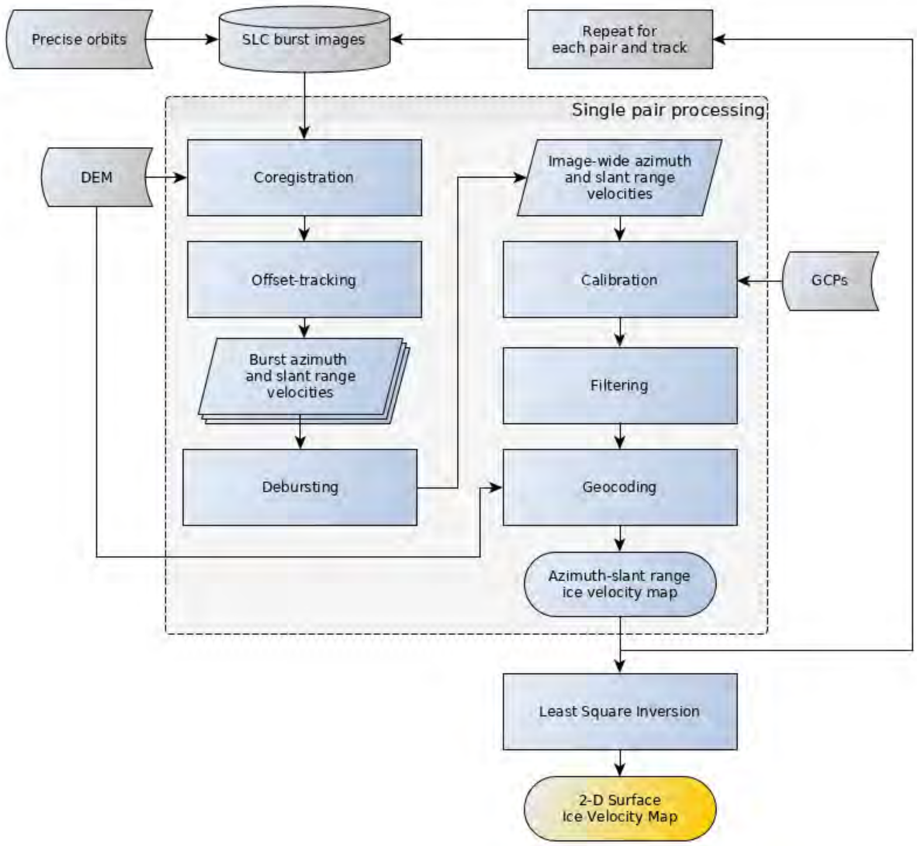

Figure 2: High-level processing flowchart for Sentinel-1 offset-tracking. GCPs: Ground Control Points. – *Yfirlit um úrvinnslu skriðhraða með hliðrunargreiningu radarmynda.*

debursted grid using a bilinear interpolation, the position of each pixel on the grid being defined by its slant-range and azimuth timing.

Because the velocity estimates obtained with offset-tracking may be biased, in particular due to changing atmospheric and ionospheric conditions, a calibration step is necessary. The calibration is performed at the track-scale, in radar geometry, against stable areas or slow-moving ground control points with known velocity. The calibrated velocity images are finally filtered for removing outliers and geocoded to a cartographic projection. In the case of Iceland, the azimuth–slant-range velocity grid is resampled to a polar stereographic projection with 100 m pixel spacing. This procedure is repeated for each 6 and 12-day pair available along the tracks covering Iceland.

The quality of the offset-tracking measurements can be degraded by changing surface conditions such as snowfall, snow melt or snow drift, that affect the radar backscatter signal, obscure features and reduce the signal-to-noise ratio of the correlation peak. It is also affected by ionospheric scintillations that can introduce local errors of several centimeters per day, observed as streaks in the velocity field. Furthermore, given the medium-resolution pixel size of S-1 acquisitions, offset-tracking performs poorly at capturing slow-moving areas (offsets of only a few centimetres).

In order to reduce noise and improve the spatial coverage, the individual 6/12-day offset-tracking results from different dates and tracks are merged to produce monthly, annual and multi-annual mosaics of the ice-velocity field over Iceland. The individual azimuth–slant-range velocity maps are combined on a pointwise basis using a least-square inversion that accounts for the transformation from the radar geometry to the cartographic reference system and assuming surface-parallel flow (Andersen *et al.*, 2020). The final products are monthly, annual or multi-annual average (in the least-square sense) 2D surface-velocity fields at 100 m resolution. Along with the ice-velocity fields, uncertainty maps are provided for both horizontal components based on the standard deviation.

RESULTS

A multi-annual weighted-average ice-velocity mosaic for the period November 2014 to December 2020 covering the Icelandic glaciers (Figure 3) derived from S-1 radar data was computed as the weighted least-squares solution from the available 6/12-day repeat maps. This weighted-average ice-velocity map is available through Wuite et al. (2021) and also, complemented with annual and monthly ice-velocity fields (Figure 4), through the ENVEO Cryoportal (http://cryoportal.enveo.at/; registration required). It should be noted that due to the varying seasonal coverage of the S-1 ice-velocity data, the ice-velocity mosaic does not represent a uniformly weighted time-average over the period 2014–2020. Data gaps are most frequent during summer when the ice velocity may be expected to be highest, so the ice-velocity mosaic likely under-represents the true time-averaged ice velocity to some degree. This needs to be kept in mind if this ice-velocity field is used in modelling studies or for other applications. The fastest ice flow, with velocities up to a few m d^{-1} or 400–800 metres per year, occurs in the lower accumulation area and the ablation area of the main outlet glaciers of the largest ice caps (Figure 3) that span a large elevation range in the areas of highest precipitation in S- and SE-Iceland. Lower velocities, on the order of a few tens of metres per year, and up to 50–100 metres per year, are observed on the large surge-type outlet glaciers of N- and W-Vatnajökull, on N-Mýrdalsjökull, Eyjafjallajökull and generally on glaciers in the central Icelandic highland and in the northern and western part of the country. The lowest velocities are, as expected, observed along the main ice divides and near the glacier margins.

Figure 4 shows the merged and averaged monthly mosaics covering Iceland for the period January 2015 to December 2020. Because offset-tracking efficiency is limited by a number of factors such as precipitation, snowmelt and snow drift caused by wind, the spatial coverage of ice-velocity maps for the glaciers varies over time. As a consequence of variations with time in the radar-image texture due to surface melting, summer months have a reduced coverage over the ice caps, even though there is in general low noise level in ice-free areas during summer due to the absence of snow. The best coverage over the glaciers is usually achieved in winter and/or early spring, depending on weather conditions, and also in late summer in some ablation areas with extensive crevassing. The coverage over ice caps improves from 2017 onward, as data availability increases and the repeat-pass period is reduced to 6 days following the launch of S-1B. Variations in noise level due to variations in coverage are the cause of changes in the hue of the images between light and darker blue and green colours in 2015–2017.

As examples, Figures 5 and 6 show in more detail the monthly weighted-average ice-velocity fields for January to December 2020. There are substantial data gaps at intermediate and high elevations in March and April on all the main ice caps, except for the April coverage on Hofsjökull which is almost complete. The coverage is temporarily improved in May, but in June and July most of the glaciers are without coverage except for a narrow elevation band near the termini where thinner snow and crevasse fields enable the identification of features that can be traced over the 6- and 12-day separation period of the radar images. The coverage starts to improve in August and is fairly complete in September and October but deteriorates in November except for Langjökull, which retains an almost complete coverage in November. The December 2020 coverage is again quite good for Vatnajökull, but substantial gaps remain in the accumulation areas of the other main ice caps in that month. The poor coverage during the summer months is presumably due to wetting of the snow pack as well as surface melting, both of which alter or destroy the features in the radar-image texture that are tracked to estimate ice velocity.

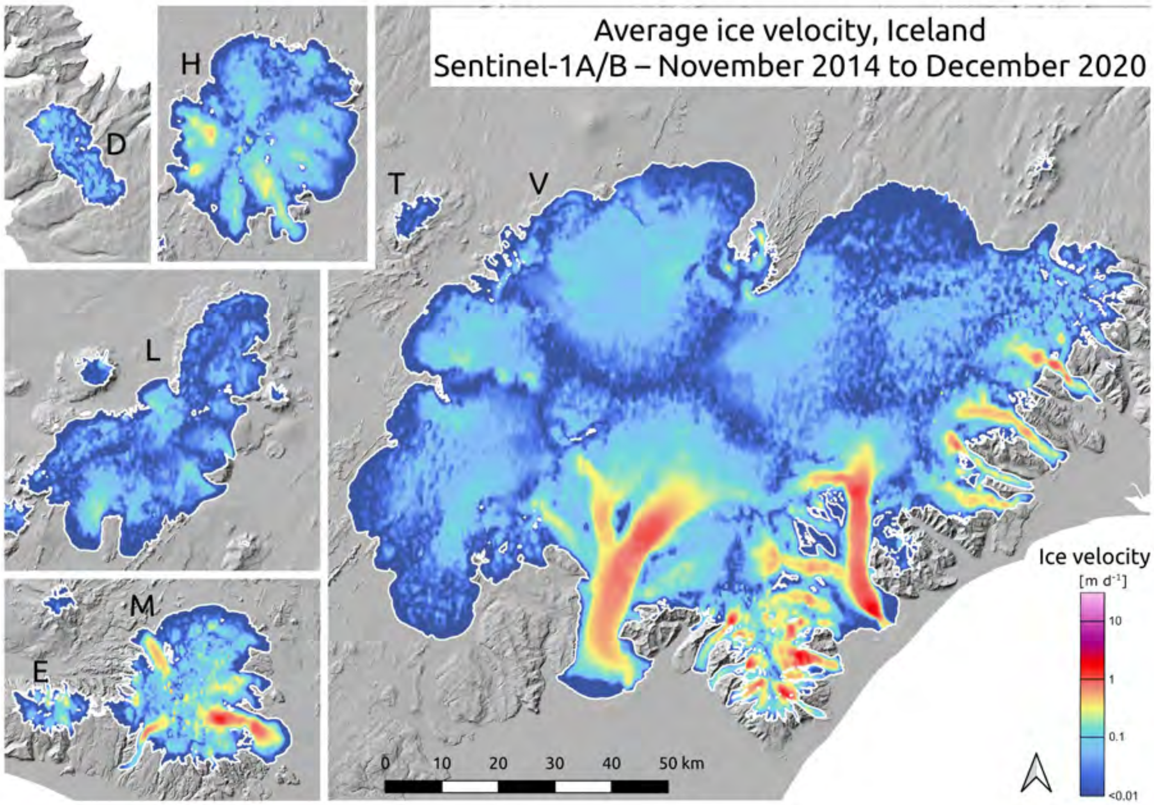

Figure 3: Weighted-average ice-flow velocity of the main ice caps in Iceland for the period November 2014 to December 2020 derived using Copernicus Sentinel-1A/B (logarithmic scale). Glacier outlines in $\sim$2000 from Sigurðsson *et al.* (2017) are shown in white. V=Vatnajökull, L=Langjökull, H=Hofsjökull, M=Mýrdalsjökull, D=Drangajökull, E=Eyjafjallajökull, T=Tungnafellsjökull. Background shading is based on lidar maps of the Icelandic glaciers from 2007–2013 (Jóhannesson *et al.*, 2013) and the ÍslandsDEM, v.1.0, from the National Land Survey of Iceland. – *Meðaltal skriðhraða íslenskra jökla frá nóvember 2014 til desember 2020, á grundvelli hliðrunargreiningar á radarmyndum Copernicus Sentinel-1A/B gervitunglanna. Jökuljaðrar um það bil árið 2000 eru með hvítri línu. Bakgrunnsskygging er byggð á leysikortum af jöklunum frá 2007–2013 (Jóhannesson o.fl., 2013) og landlíkani af Íslandi frá Landmælingum Íslands.*

Ice-flow velocity profiles near the termini of outlet glaciers of S-Vatnajökull

As an example of the potential of the ice-velocity data set for areas with the best coverage, Figure 7 shows velocity profiles near the termini of the outlet glaciers Skeiðarárjökull, Breiðamerkurjökull, and Morsárjökull, Skaftafellsjökull and Svínafellsjökull (the last three are shown together in the last row of the figure) in S-Vatnajökull.

There is seasonal variation in the ice-flow velocity, with the highest velocity during spring/summer and lowest velocity in winter for all five glaciers. The profiles also clearly show the sharp boundaries of the ice-flow channels with high velocity and most of the velocity increase at the boundaries taking place over distances of $\sim$1–2 km.

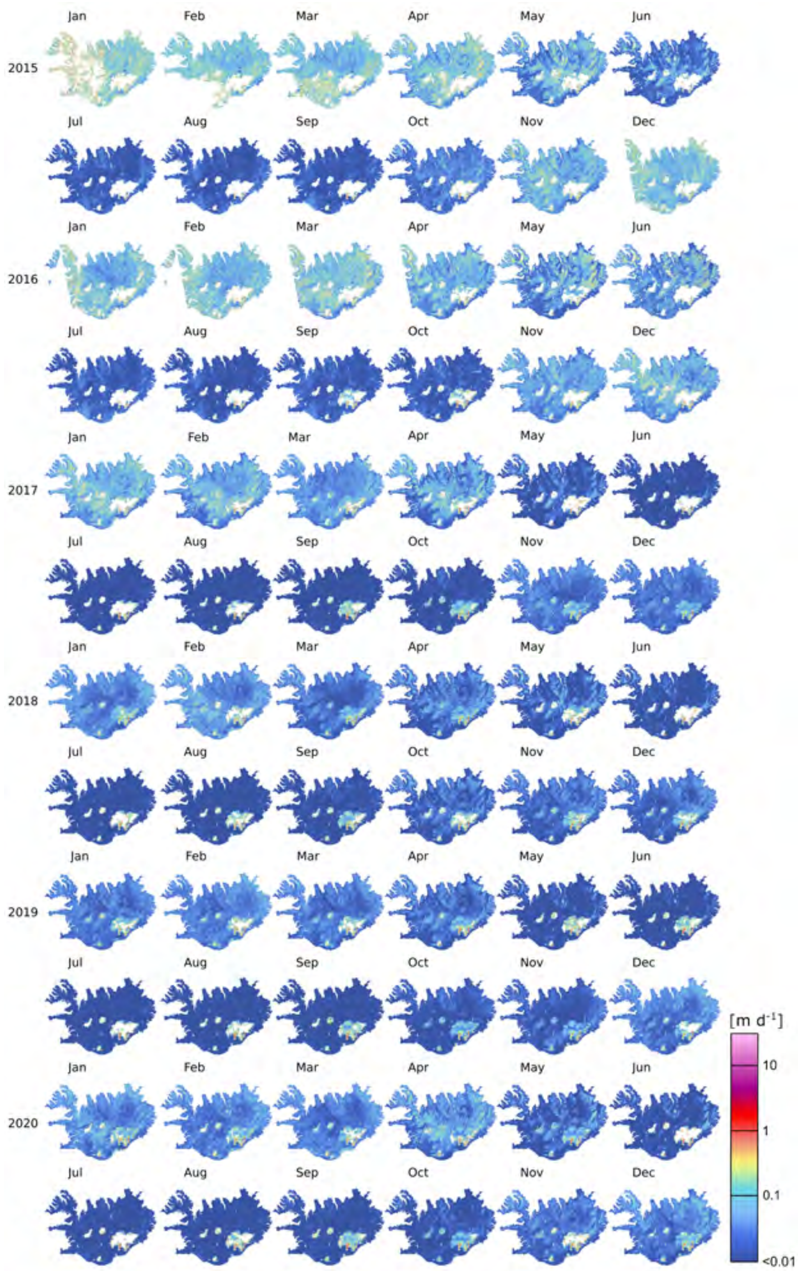

Figure 4: Monthly velocity maps for Iceland derived from Sentinel-1A/B radar images, January 2015 to December 2020 (logarithmic scale). The monthly panels are mainly intended to give an overview of variations in data coverage with time, in particular over the glaciers, rather than a quantitative representation of the derived ice-velocity fields, which are depicted in the following figures. – *„Meðalhraði" yfirborðshreyfingar á Íslandi reiknaður á grundvelli Sentinel-1A/B radarmynda fyrir hvern mánuð ársins á tímabilinu janúar 2015 til desember 2020.*

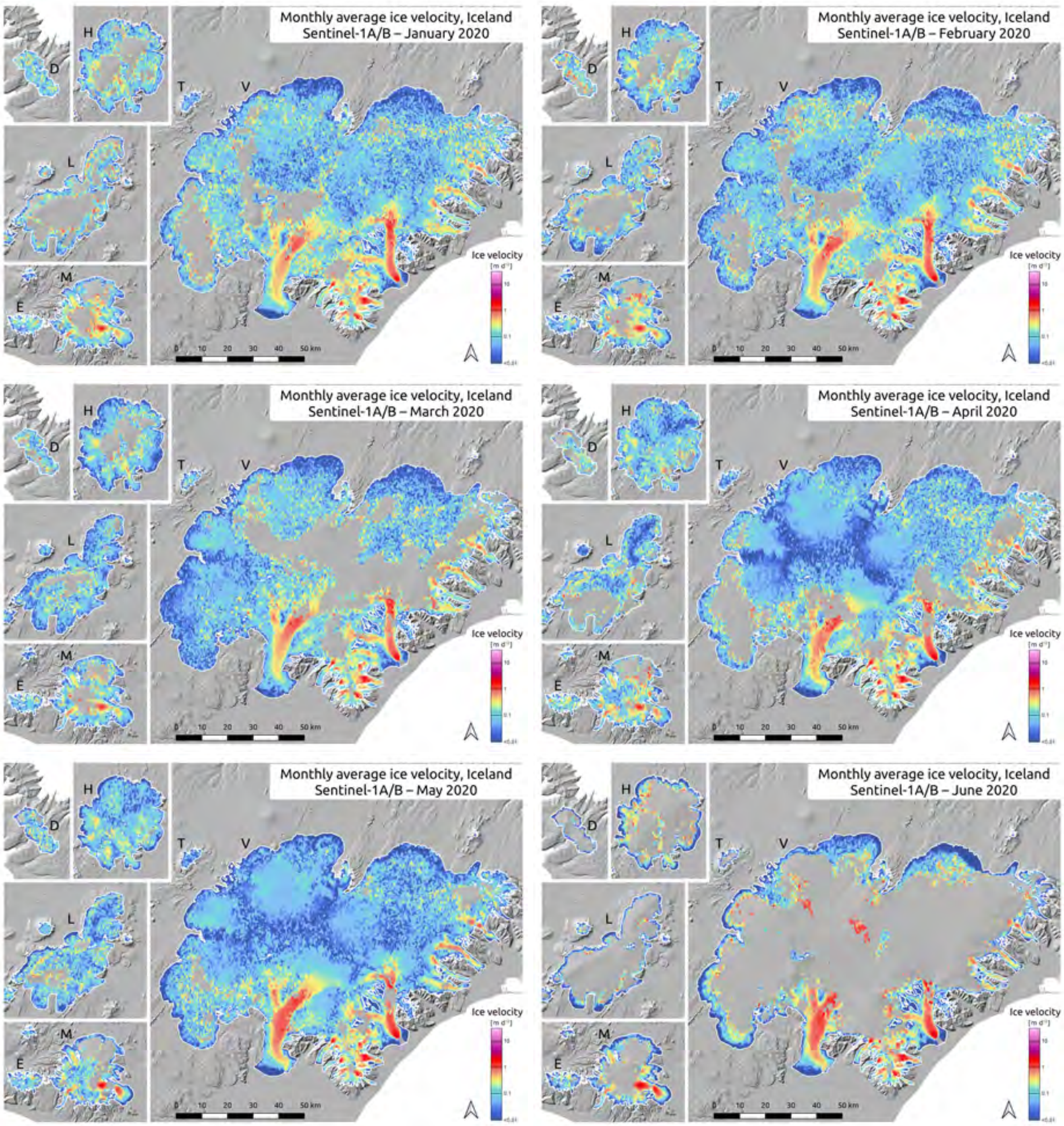

Figure 5: Weighted-average ice-flow velocity of the main ice caps in Iceland for the months January to June 2020 derived by offset-tracking of Sentinel-1A/B radar images. For explanations and credits see the caption of Figure 3. – *Meðaltal skriðhraða fyrir íslenska jökla fyrir mánuðina janúar til júní 2020 á grundvelli hliðrunargreiningar á Sentinel-1A/B radarmyndum. Sjá nánari skýringar við 3. mynd.*

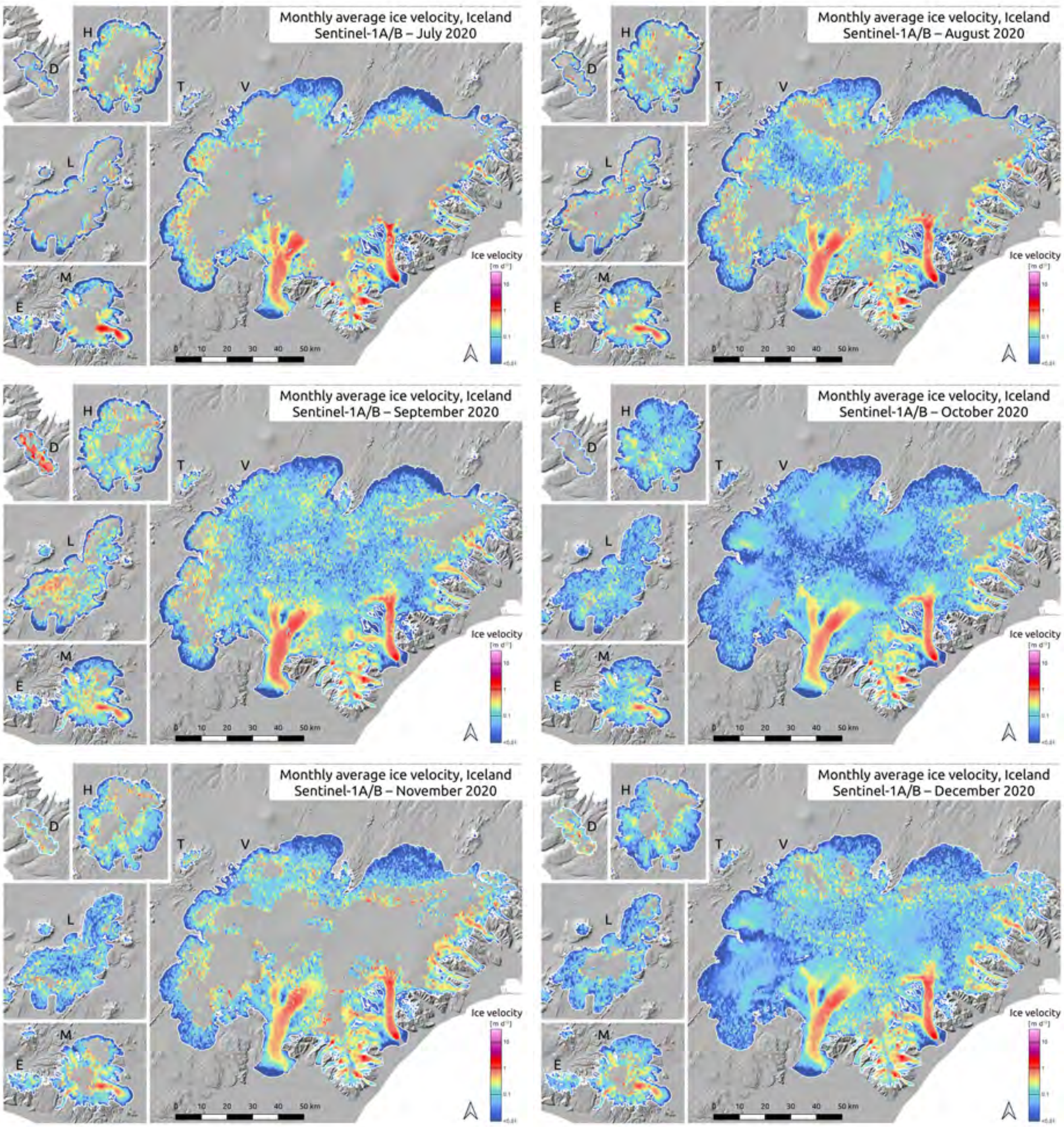

Figure 6: Weighted-average ice-flow velocity of the main ice caps in Iceland for the months July to December 2020 derived by offset-tracking of Sentinel-1A/B radar images. For explanations and credits see the caption of Figure 3. – *Meðaltal skriðhraða fyrir íslenska jökla fyrir mánuðina júlí til desember 2020 á grundvelli hliðrunargreiningar á Sentinel-1A/B radarmyndum. Sjá nánari skýringar við 3. mynd.*

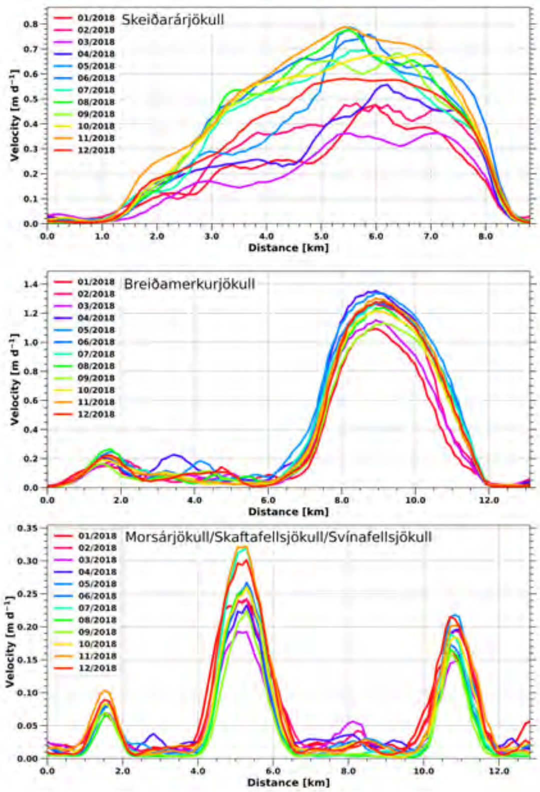

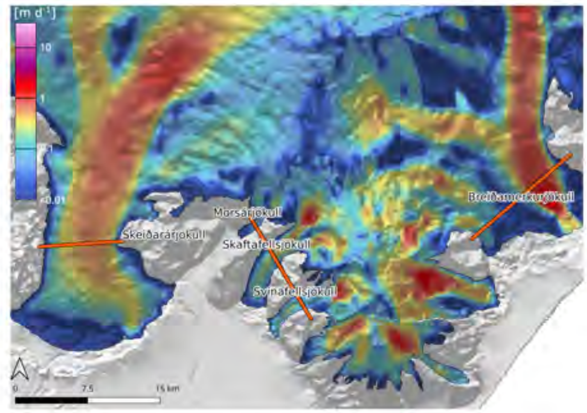

Figure 7: Left: Cross-profiles of monthly ice-flow velocity in 2018 for five outlet glaciers in S-Vatnajökull, derived by offset-tracking of Sentinel-1A/B radar images. Right: The location of the profiles shown with red lines on the 2014–2020 weighted-average ice-flow velocity field. – *Skriðhraðaþversnið fyrir Skeiðarárjökul (efst), Breiðamerkurjökul (mið) og Morsárjökul/Skaftafellsjökul/Svínafellsjökul (neðst) fyrir árið 2018 á grundvelli hliðrunargreiningar á Sentinel-1A/B radarmyndum. Staðsetning sniðanna er sýnd með rauðum línum á kortinu til hægri með meðalskriðhraða áranna 2014–2020 sem bakgrunn.*

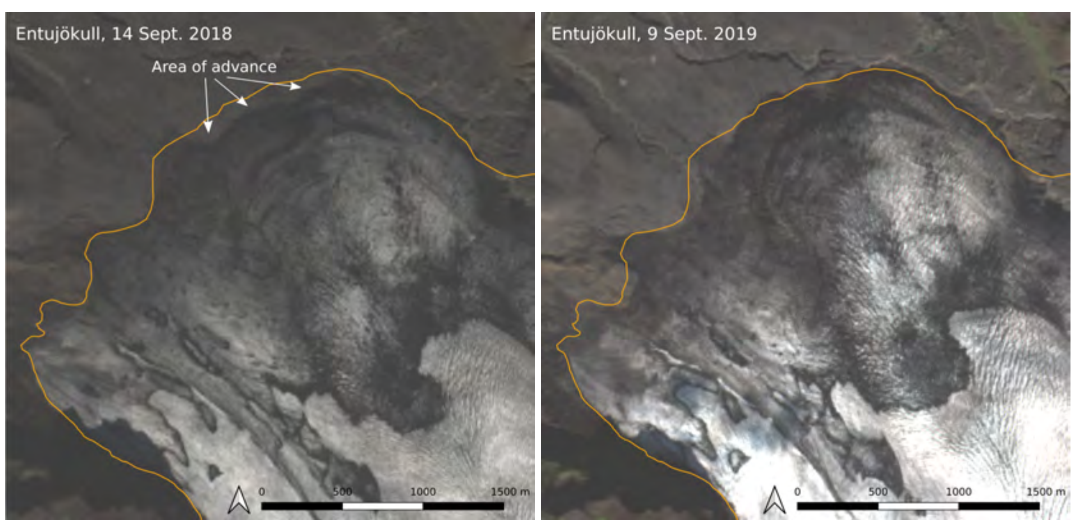

Figure 8: Sentinel-2 satellite images of Entujökli from 14 September 2018 (left) and 9 September 2019 (right) showing an advance of the eastern part of the glacier terminus over this time period. Glacier outlines in 2019 from Hannesdóttir *et al.* (2020) are shown in yellow. The area of advance is indicated with arrows on the 2018 image. *Sentinel-2 gervihnattamyndir af Entujökli frá 14. september 2018 (til vinstri) og 9. september 2019 sem sýna að austurhluti jökulsins gekk fram milli þess sem þessar myndir voru teknar. Jökuljaðarinn árið 2019 er sýndur með gulri línu. Svæðið þar sem jökullinn gekk fram er sýnt með örvum á myndinni frá 2018.* Image processing/myndvinnsla: Ragnar H. Þrastarson.

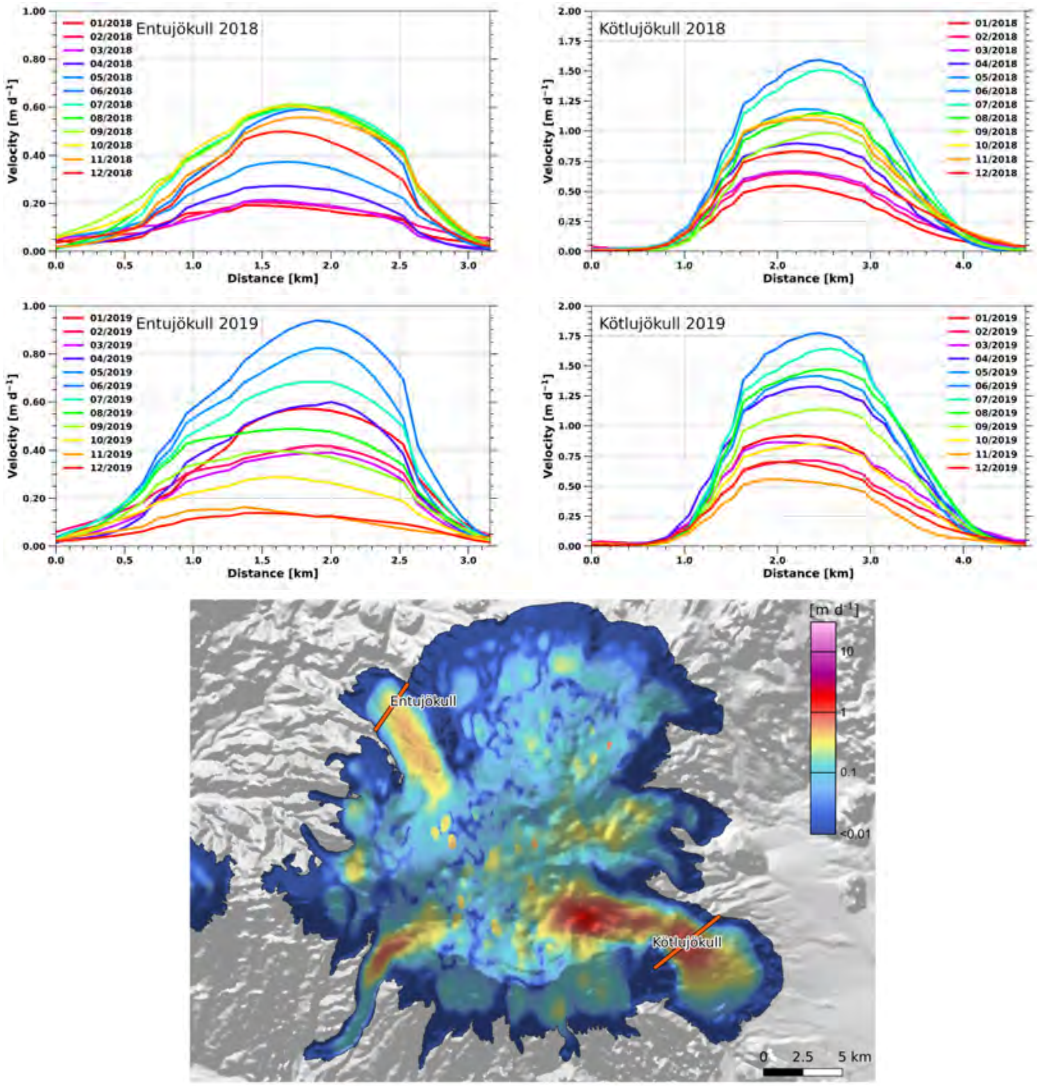

Figure 9: Cross-profiles of monthly ice-flow velocity for the outlet glaciers Entujökull (the two panels in the left column) and Kötlujökull (the two panels in the right column) in Mýrdalsjökull ice cap for 2018 and 2019 derived by offset-tracking of Sentinel-1A/B radar images (note the different vertical scales for the two glaciers). An advance of terminus of Entujökull in early 2019 was associated with a increase in winter ice velocities. The location of the profiles is shown with red lines on the map in the lowest panel with the 2014–2020 weighted-average ice-flow velocity field as background. – *Skriðhraða-þversnið fyrir Entujökul (tvær myndir vinstra megin) and Kötlujökul (tvær myndir hægra megin) í Mýrdalsjökli fyrir árin 2018 og 2019 á grundvelli hliðrunargreiningar á Sentinel-1A/B radarmyndum. Entujökull gekk fram árið 2019. Staðsetning sniðanna er sýnd með rauðum línum á kortinu í neðstu myndaröðinni með meðalskriðhraða áranna 2014–2020 sem bakgrunn.*

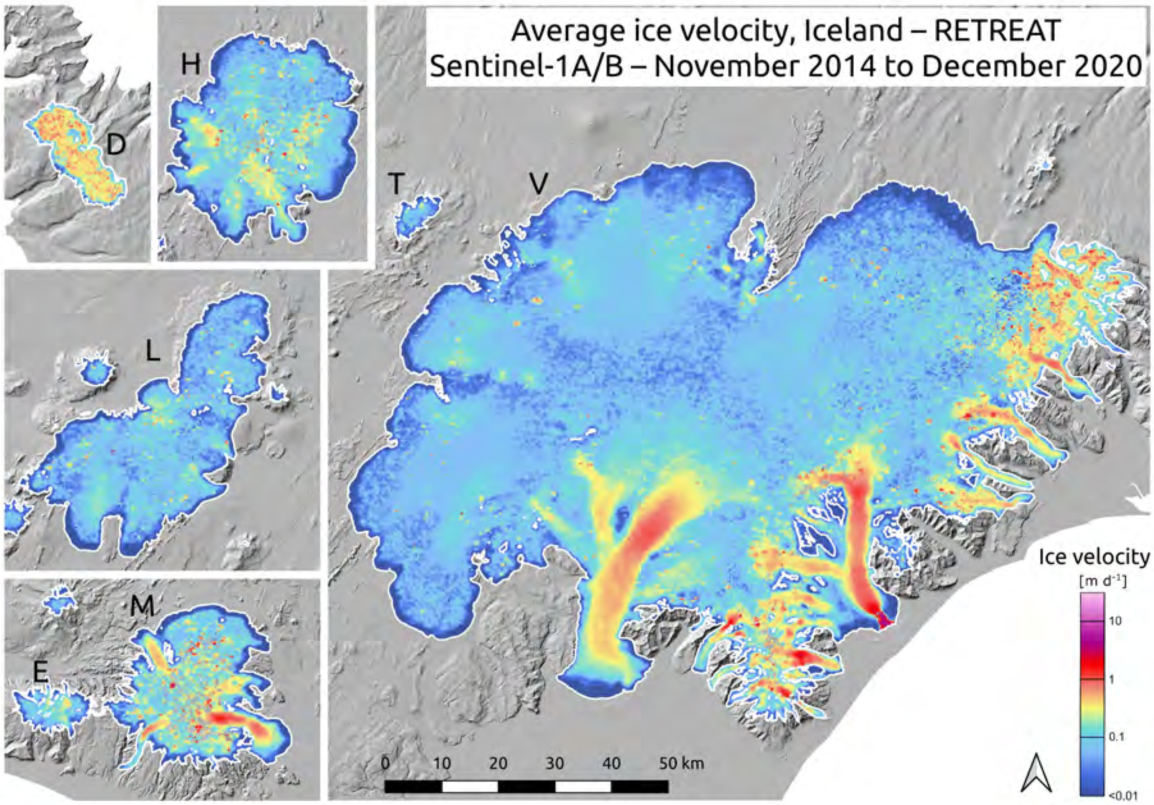

Figure 10: Average ice-flow velocity of the main ice caps in Iceland derived by offset-tracking of Sentinel-1 radar images and provided by the RETREAT project (Friedl *et al.*, 2021). For explanations and credits see the caption of Figure 3. – *Meðaltal skriðhraða fyrir íslenska jökla á grundvelli hliðrunargreiningar á Sentinel-1 radar gervihnattamyndum á tímabilinu nóvember 2014 til desember 2020 úr RETREAT verkefninu (Friedl o.fl., 2021). Sjá nánari skýringar við 3. mynd.*

Late-winter speed-up in Entujökull in 2019

The northern part of the terminus of Entujökull in N-Mýrdalsjökull advanced in 2019 by 100–200 m with respect to its position in the previous year (see Figure 8). Figure 9 (left panels) shows that the ice-flow velocity of this glacier was substantially higher in early 2019 than in 2018 (and also with respect to the years 2016, 2017 and 2020, not shown), and that similar differences between these years in terms of magnitude and seasonality are not as noticeable on the Kötlujökull outlet glacier of the same ice cap (Figure 9, right panels), neither at the locations of the profiles in Figure 9 nor at other elevations (not shown). A clear seasonal variation in the ice-flow velocity is seen for both glaciers as was the case for the outlet glaciers of Vatnajökull discussed in the previous subsection (Figure 7). The speed-up event in Entujökull in 2019 took place during late winter and was characterized by a distinct change in the seasonality of the ice-flow velocity, which typically reaches a seasonal maximum during summer. In this sense, it is different from recent advances of several termini of steep outlet glaciers in S- and SE-Iceland (Hannesdóttir, 2020), that are observed to advance in connection with a general increase in the ice-flow velocity over the entire year, or of a smaller magnitude than for Entujökull.

Interestingly, the upper limit of the speed-up area on Entujökull in the spring of 2019 is at the location of two ice-surface cauldrons, MY-21 and MY-22, which release regular jökulhlaups in middle or late summer. The cauldrons did, however, not release a significant flood in early 2019 (Magnússon, pers. comm., Feb. 2022). The 2019 speed-up and the associated advance of the terminus may have been caused by a small surge of the Entujökull outlet glacier, which is, however, not previously known to be a surge-type glacier (Björnsson *et al.*, 2003). Surges are often observed to start during the winter months as discussed by Raymond (1997), although this is by no means a fixed rule.

Comparison with other ice-velocity data sets for Icelandic glaciers based on radar and optical images

We compared the S-1-based weighted-average ice-velocity mosaic in Figure 3 with the global RETREAT ice-velocity data set, which is also based on offset-tracking of S-1 radar images (Friedl *et al.*, 2021) (Figure 10), and with ice velocities generated using Landsat optical images and provided by the NASA MEaSUREs ITS_LIVE project (Gardner *et al.*, 2021) (Figure 11). Overall there is good agreement between the three data sets in terms of the location and magnitude of the main ice-flow channels and other spatial ice-velocity patterns. It should be noted that none of these data sets represents a uniformly weighted time-average over the period in question, so detailed quantitative agreement should not be expected.

Comparison of the S-1-derived ice-velocity fields presented in this paper with the fields provided by the RETREAT project based on the same satellite radar images reveals a greater number of scattered outliers and irregularities in the RETREAT velocity over the accumulation areas, in particular for the Drangajökull ice cap for which the comparatively large magnitude and short-scale spatial variations of the RETREAT velocity field in the area of the main SW–NE ice-divide of the ice cap seem implausible. The RETREAT velocity field is also consistently higher along the ice divides of the other main Icelandic ice caps. The same tendency for higher velocities in the RETREAT data is seen near the ice margin in the ablation areas of all the main ice caps. As near-zero ice velocity is expected in ice-divide areas where the ice motion changes direction between adjacent ice-flow basins, the observed differences along the ice-divides indicate a high-bias in low-velocity areas in the RETREAT data set. Figures 3 and 10 combine data from the entire period 2014 to 2020 and thereby achieve almost 100 % coverage over the glaciers for both data sets in spite of large areas without data in the individual monthly velocity fields (cf. Figures 5 and 6). Table 1 summarizes the proportional data coverage for the monthly ENVEO and RETREAT ice-velocity data sets for the year 2020, showing that the areas with valid velocity are larger in the ENVEO data set for all months of this year, with more than twice as large areas in the ENVEO data for the months of January, September and November compared with the RETREAT data.

Comparison between the S-1-based ice-velocity fields presented in this paper and by the RETREAT project with the ITS_LIVE date set shows that the ice velocity derived from optical data is affected by a larger number of outliers and gaps as discussed in more detail by Friedl *et al.* (2021), particularly in the accumulation area of the largest ice cap, Vatnajökull, but also to a lesser degree on other glaciers. There are almost no valid ITS_LIVE ice velocities on Drangajökull ice cap, on the NW-peninsula, and on the outlet glaciers in SE-Vatnajökull where data are also missing. We did not make a similar comparison of the ice-velocity fields presented in this paper to the GoLIVE ice-velocity data set (Fahnestock *et al.*, 2015), which is generated using Landsat optical images as the ITS_-LIVE velocity, since a detailed comparison by Friedl *et al.* (2021) shows that the ITS_LIVE and GoLIVE ice velocities are rather similar in terms of coverage and error characteristics.

Figure 12 shows for comparison the 2018 annual ice-velocity fields of Vatnajökull from the two S-1 data sets and the ITS_LIVE data set and two velocity profiles taken along the center flowlines of Skeiðarárjökull and Breiðamerkurjökull, and extended across the ice divide, from these three data sets. As can be seen, the optical data set is affected by a larger number of outliers, but the profile shapes generally agree although differences in velocity can exceed 10–15 cm d^{-1} on Skeiðarárjökull. The differences in data

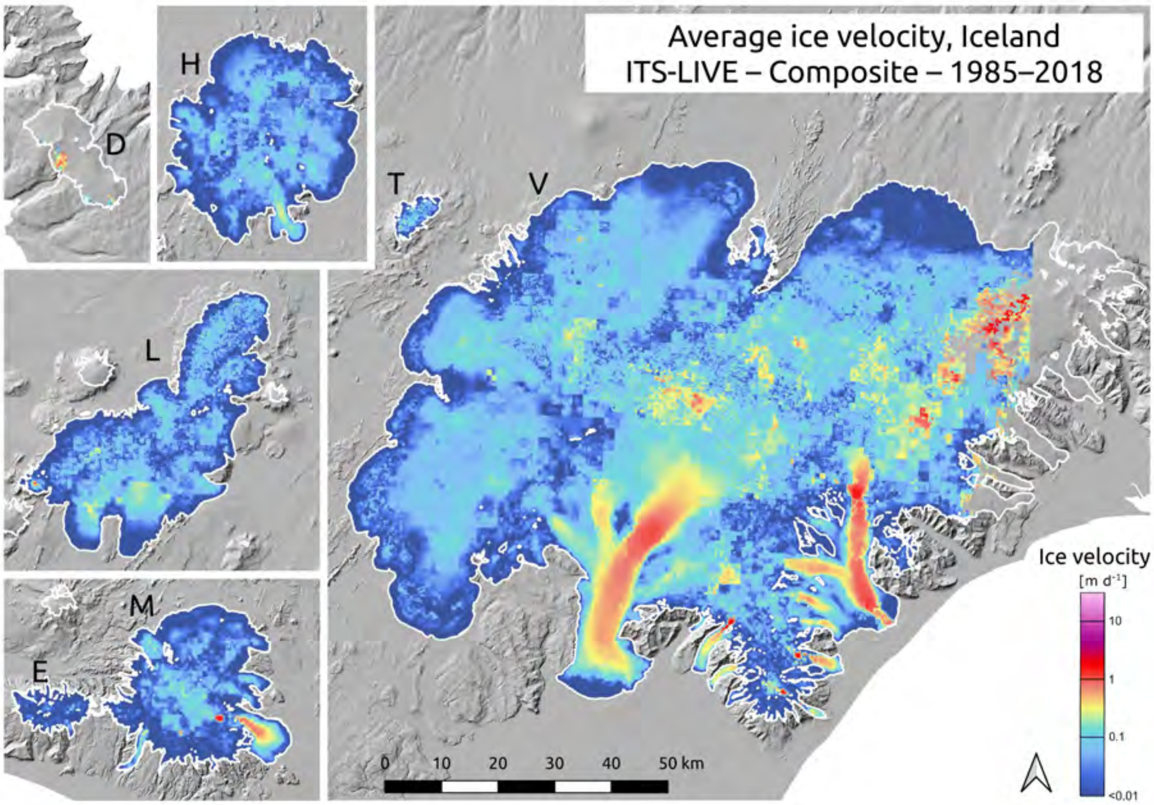

Figure 11: Weighted-average ice-flow velocity of the main ice caps in Iceland derived by offset-tracking of Landsat images from the period 1985–2018 provided by the NASA MEaSUREs ITS_LIVE project (Gardner et al., 2021). For explanations and credits see the caption of Figure 3. – *Meðaltal skriðhraða fyrir íslenska jökla á grundvelli hliðrunargreiningar á Landsat gervihnattamyndum frá tímabilinu 1985 til 2018 (Gardner o.fl., 2021). Sjá nánari skýringar við 3. mynd.*

Table 1: Proportional data coverage for the monthly ENVEO and RETREAT Sentinel-1 ice-velocity data sets for the Icelandic glaciers in 2020. – *Hlutfall svæða með mánaðarlegum gögnum í ENVEO and RETREAT hraðagreiningum fyrir íslensku jöklana árið 2020.*

Data set	**Jan.**	**Feb.**	**Mar.**	**Apr.**	**May**	**June**	**July**	**Aug.**	**Sep.**	**Oct.**	**Nov.**	**Dec.**
ENVEO	86	88	81	88	96	42	49	68	90	96	68	94
RETREAT	33	60	48	56	67	31	28	39	40	73	30	54

coverage may partly reflect a fundamental difference in the suitability of optical versus SAR data for ice-velocity retrieval. The profiles also show the consistently higher values found along the ice-divides in the RETREAT and ITS_LIVE datasets where near-zero ice velocity is expected.

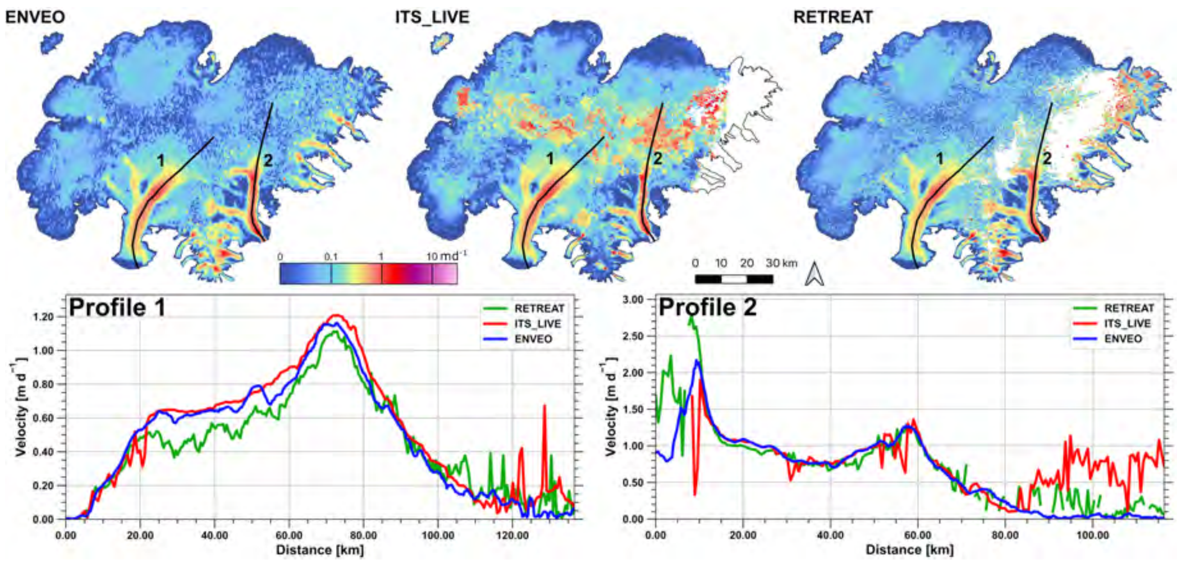

Figure 12: Ice-flow velocity of Vatnajökull in 2018 derived in this study (left), from Landsat optical images from the ITS_-LIVE project (Gardner et al., 2021) (centre) and from RETREAT (Friedl *et al.*, 2021) (right). The black lines show the location of the two profiles depicted below the velocity maps. – *Skriðhraði íss á Vatnajökli árið 2018 skv. greiningunni sem hér birtist (til vinstri), ITS_LIVE hraði sem reiknaður er með hliðrunargreiningu á Landsat gervihnattamyndum (Gardner o.fl., 2021) (í miðju) og skv. greiningu Friedl o.fl. (2021) sem einnig byggir á Sentinel-1 radar gervihnattamyndum (til hægri). Svartar línur á kortunum sýna staðsetningu hraðasniða á neðri hluta myndarinnar.*

DISCUSSION AND CONCLUSION

The initial results, presented here, from producing regular ice-velocity fields for the Icelandic glaciers based on Copernicus Sentinel-1 radar images show that these data have a large potential for studying and monitoring ice dynamics, both general features of the ice-flow field in terms of spatial and seasonal variations in ice velocity and for studying events such as surges and jökulhlaups. In combination with regular, repeat ice-surface mapping (e.g. Hugonnet *et al.*, 2021), the remotely-sensed ice velocity enables detailed analysis of many glaciological phenomena where lack of data has prevented detailed studies of the underlying glaciological dynamics. Dehecq *et al.* (2019) show that changes in ice-flow velocity in the ITS_LIVE data set are intimately connected with long-term ice-thickness changes for glaciers in High Mountain Asia so monitoring of changes in ice-flow velocity are likely to become an integral part of the monitoring of glacier mass balance and studies of the effect of changes in climate on glaciers in the future.

In terms of long-term average ice velocity, the results reveal a consistent spatial pattern with distinct channelled ice flow within many of the main outlet glaciers. The overall agreement of this pattern with the long-term average ITS_LIVE ice-flow velocity field, derived from Landsat optical images, indicates that this pattern is realistically captured by both satellite data sets. The ice-velocity field derived from the Sentinel-1 radar images is, however, less affected by outliers and has a better spatial and temporal coverage as discussed by Friedl *et al.* (2021).

Seasonal data gaps in the Sentinel-1 radar velocity data set may result in biases in the long-term average ice velocity because of seasonal ice-velocity variations (cf. Figures 7 and 9) and will lead to bias at locations where data from some times of the year are always or almost always missing. This source of bias needs to be kept in mind in the use of the data.

The loss of coverage because of decorrelation over the 6- and 12-day interval between images currently prevents study of ice-flow variations over days, weeks and months for most of the ice caps, except for the ablation areas of many outlet glaciers where ice-flow variations are captured with good time resolution (cf. Figures 7 and 9). This limits the potential of the ice-velocity data for the study of surges and jökulhlaups to some extent but it remains to be seen whether adaptation to Icelandic conditions in the offset-tracking processing can be used to improve the data coverage. In spite of the extensive data gaps, the current data coverage in the ablation areas and during most winter months will provide interesting data to shed light on the dynamics of some surges and jökulhlaups. Potential processing improvements that are being studied are: (1) improvements for slow-moving ice areas by accounting for lowering of the glacier surface due to ablation using an ice ablation model, (2) better treatment of ionospheric effects, and (3) use of Sentinel-1 Extended Timing Annotation Dataset (ETAD) with improved geometric accuracy (Gisinger et al., 2021). The usefulness of Sentinel-1 ice-velocity observations for jökulhlaup studies is mainly related to the effect of the floods on ice-dynamics over the subglacial flood path. The jökulhlaup-induced ice motion over the subglacial source area consists mainly of vertical motion that it not captured in the Sentinel-1 offset-tracking velocities.

The ice-velocity data set provides useful input and validation data for ice-flow modellers studying the Icelandic glaciers. The velocity data may also be useful for mass-balance studies where the observed surface velocity can be compared with an estimate of the balance velocity (Cogley *et al.*, 2011) to assess the degree of disequilibrium of different ice-flow basins, for example for studying the build-up of outlet glaciers towards a surge and the effect of ongoing climate warming on glacier mass balance and ice dynamics. The ice-velocity fields, furthermore, have potential usefulness for monitoring changing horizontal velocity patterns in the neighbourhood of high-temperature geothermal areas, subglacial volcanic vents and where retreating termini calve into proglacial lakes. Changing velocity patterns due to variations in subglacial hydrology, for example at the onset of the melt season, provide yet another interesting subject for study. These are just a few examples of the potential usefulness of the ice-velocity data. As with all new remote-sensing glaciological data sets, more potential applications may be expected to emerge after the data are further applied in scientific studies.

Data availability

A digital data set with the 2014–2020 average ice velocity derived in this research is available in the open-access Zenodo repository (https://doi.org/10.5281/-zenodo.5517241; Wuite *et al.*, 2021). Annual and monthly ice-velocity fields, which will be regularly updated, are freely available through the ENVEO Cryoportal (http://cryoportal.enveo.at; registration required). The RETREAT Sentinel-1 (Friedl *et al.*, 2021) and NASA MEaSURE ITS_LIVE Landsat-8 (Gardner *et al.*, 2021) ice-surface velocity products are available via interactive web portals at http://retreat.geographie.uni-erlangen.de and https://-doi.org/10.5067/6II6VW8LLWJ7, respectively.

Acknowledgements

This study was supported by the Icelandic Research Fund, grant number 206770-051. We thank Eyjólfur Magnússon for providing information about cauldrons in Mýrdalsjökull.

ÁGRIP

Radarmyndir úr gervihnöttum sýna breytilegt endurkast frá yfirborði jarðar sem endurspeglar óreglur í ýmsum eiginleikum efstu jarðlaga. Þar sem hreyfing er á lausum jarðlögum eða jöklum er unnt er að meta hraða hreyfingarinnar með því greina hliðrun í endurkastsmynstri milli radarmynda frá mismunandi tímum og nefnist aðferðin „offset-tracking“ á ensku. Nú er unnt að mæla yfirborðshraða ísskriðs á reglulegu neti yfir heilu jöklana með nokkurra daga eða vikna millibili og fylgjast með breytingum ísskriðsins í tíma og rúmi. Íslensku jöklarnir bjóða upp á einstætt tækifæri til þess að beita þessari nýju tækni. Margvísleg gögn eru tiltæk úr fyrri rannsóknum, auðvelt aðgengi er að jöklunum til mælinga, og jökulhlaup og framhlaup, sem reglulega verða í jöklunum, bjóða upp á fjölmörg áhugaverð rannsóknarefni. Evrópsku Copernicus Sentinel-1 gervitunglin hafa tekið radarmyndir af Íslandi á 6 eða 12 daga fresti síðan haustið 2014. Hliðrunargreiningu hefur verið beitt til þess að greina skriðhraða jökla hér á landi í íslensk–austurrísku rannsóknarverkefni sem stutt er af Rannís. Hliðstæð greining hefur verið unnin fyrir ísbreiður Grænlands og Suðurskautslandsins og ýmsa aðra jökla jarðar á síðustu árum. Meðalskriðhraði íslensku jöklanna samkvæmt frumniðurstöðum þessara rannsókna er langmestur um miðbik og neðarlega í skriðjöklum sem spanna mikið hæðarbil á landsvæðum þar sem mikil úrkoma fellur. Þar getur hraðinn verið 400–800 metrar á ári þar sem hann er mestur á Skeiðarárjökli, Breiðamerkurjökli og Kötlujökli. Hraðinn er einnig tiltölulega mikill á skriðjöklum Öræfajökuls og á skriðjöklum í suðaustanverðum Vatnajökli, mun meiri en á stóru skriðjöklunum í norðan- og vestanverðum Vatnajökli. Þar mælist hraðinn víða nokkrir tugir metra á ári og upp í 50–100 metra á ári og svipaður hraði mælist á jöklum á miðhálendinu og á Vesturlandi og Vestfjörðum. Einnig má sjá að jökulísinn skriður mjög hægt í grennd við ísaskil og víðast nærri jöðrum jöklanna. Hliðrunargreiningin gefur ekki alltaf fullnægjandi niðurstöður fyrir blautan vetrarsnjó að vor- og sumarlagi eða fyrir jökulís á sprungulitlum leysingarsvæðum að sumri. Greiningin gengur hins vegar oftast vel fyrir kaldan vetrarsnjó og fyrir leysingarsvæði þar sem nokkuð er um sprungur.

REFERENCES

Aðalgeirsdóttir, G., E. Magnússon, F. Pálsson, Th. Thorsteinsson, J. M. C. Belart, T. Jóhannesson, H. Hannesdóttir, O. Sigurðsson, A. Gunnarsson, B. Einarsson, E. Berthier, L. Steffensen Schmidt, H. H. Haraldsson and H. Björnsson 2020. Glacier changes in Iceland in the 20^{th} and the beginning of the 21^{st} century. *Front. Earth Sci.* 8, 523646. https://doi.org/10.3389/-feart.2020.523646

Andersen, J. K., A. Kusk, J. P. Merryman Boncori, C. Schott Hvidberg and A. Grinsted 2020. Improved ice velocity measurements with Sentinel-1 TOPS interferometry. *Remote Sens.* 12(12), 2014. http://doi.org/-10.3390/rs12122014

Berthier, E., H. Björnsson, F. Pálsson, K. L. Feigl, M. Lubes and F. Rémy 2006. The level of the Grímsvötn subglacial lake, Vatnajökull, Iceland, monitored with SPOT5 images. *Earth Planet. Sci. Lett.* 243, 293–302. http://doi.org/10.1016/j.epsl.2005.12.027

Björnsson, H., H. Rott, S. Gudmundsson, A. Fischer, A. Siegel and M. T. Gudmundsson 2001. Glacier-volcano interactions deduced by SAR interferometry. *J. Glaciol.* 47(156), 58–70. http://doi.org/10.3189/-172756501781832520

Björnsson, H., F. Pálsson, O. Sigurðsson and G. E. Flowers 2003. Surges of glaciers in Iceland. *Ann. Glaciol.* 36(1), 82–90. http://doi.org/10.3189/-172756403781816365

Björnsson, H. and F. Pálsson 2008. Icelandic glaciers. *Jökull* 58, 365–386.

Björnsson, H. 2009/2017. *Jöklar á Íslandi*. Reykjavík, Opna, 479. English translation: D'Arcy, J. M. 2017. *The Glaciers of Iceland: A Historical, Cultural and Scientific Overview*. Serie: Atlantis Advances in Quaternary Science v. 2. Atlantic Press, 613 pp. [In Icelandic], http://doi.org/10.2991/978-94-6239-207-6

Cogley, J. G., R. Hock, L. A. Rasmussen, A. A. Arendt, A. Bauder, R. J. Braithwaite, P. Jansson, G. Kaser, M. Möller, L. Nicholson and M. Zemp 2011. *Glossary of Glacier Mass Balance and Related Terms*. IHP-VII Technical Documents in Hydrology No. 86, IACS Contribution No. 2, UNESCO-IHP, Paris.

De Zan, F. and A. Monti Guarnieri 2006. TOPSAR: Terrain Observation by Progressive Scans *IEEE Trans. Geosc. Rem. Sens.* 44(9), 2352–2360. http://doi.org/-0.1109/TGRS.2006.873853

Dehecq, A., N. Gourmelen, A. S. Gardner, F. Brun, D. Goldberg, P. W. Nienow, E. Berthier, C. Vincent, P. Wagnon and E. Trouvé 2019. Twenty-first century glacier slowdown driven by mass loss in High Mountain Asia. *Nature Geosci.* 12, 22–27. https://doi.org/-10.1038/s41561-018-0271-9

Einarsson, B., E. Magnússon, M. J. Roberts, F. Pálsson, F., Th. Thorsteinsson and T. Jóhannesson 2016. A spectrum of jökulhlaup dynamics revealed by GPS measurements of glacier surface motion. *Ann. Glaciol.* 57(72), 47–61. http://doi.org/10.1017/aog.2016.8

ENVEO; Wuite, J., M. Hetzenecker, T. Nagler, S. Scheiblauer 2021. ESA Antarctic Ice Sheet Climate Change Initiative (Antarctic Ice Sheet CCI): Antarctic Ice Sheet monthly velocity from 2017 to 2020, derived from Sentinel-1, v1. NERC EDS Centre for Environmental Data Analysis, 28 June 2021. http://dx.doi.org/10.5285/00fe090efc-58446e8980992a617f632f

Fahnestock, M., T. Scambos, T. Moon, A. Gardner, T. Haran and M. Klinger 2015. Rapid large-area mapping of ice flow using Landsat 8. *Remote Sensing of Environment*, 185. 84–94. http://doi.org/10.1016/j.rse.-2015.11.023

Fischer, A., H. Rott and H. Björnsson 2003. Observation of recent surges of Vatnajökull, Iceland, by means of ERS SAR interferometry. *Ann. Glaciol.* 37, 69–76. http://doi.org/10.3189/172756403781815546

Friedl, P., T. Seehaus and M. Braun 2021. Global time series and temporal mosaics of glacier surface velocities derived from Sentinel-1 data. *Earth Syst. Sci. Data* 13, 4653–4675. http://doi.org/10.5194/essd-13-4653-2021

Gardner, A. S., G. Moholdt, T. Scambos, M. Fahnstock, S. Ligtenberg, M. van den Broeke and J. Nilsson 2018. Increased West Antarctic and unchanged East Antarctic ice discharge over the last 7 years. *Cryosph.* 12(2), 521–547. http://doi.org/10.5194/tc-12-521-2018

Gardner, A. S., M. A. Fahnestock and T. A. Scambos 2021 (accessed 14 May 2021). ITS_LIVE Regional Glacier and Ice Sheet Surface Velocities. Data archived at National Snow and Ice Data Center. http://doi.org/-10.5067/6II6VW8LLWJ7

Gisinger, C., T. Nagler, L. Libert, P. Marinkovic, Y. Larsen, N. Miranda, A. Valentino, H. Breit, S. Suchandt, U. Balss, L. Krieger, T. Fritz and M. Eineder 2021. Evaluation of ESA's Extended Timing Annotation Dataset (ETAD) for Sentinel-1 – First Results for Ice Velocity Monitoring and InSAR Applications in Greenland, Iceland and Norway. Abstract for FRINGE 2021 (online event), 31 May – 04 June 2021. https://elib.dlr.de/142648/

Gray, A. L., N. Short, K. E. Mattar and K. C. Jezek 2001. Velocities and flux of the Filchner ice shelf and its tributaries determined from speckle tracking interferometry. *Canadian J. Rem. Sens.* 27(3), 193–206. http://-doi.org/10.1080/07038992.2001.10854936

Guðmundsson, S., M. T. Gudmundsson, H. Björnsson, F. Sigmundsson, H. Rott and J. M. Carstensen 2002. Three-dimensional glacier surface motion maps at the Gjálp eruption site, Iceland, inferred from combining InSAR and other ice displacement data. *Ann. Glaciol.* 34, 315–322. http://doi.org/10.3189/-172756402781817833

Hannesdóttir, H., O. Sigurðsson, R. H. Þrastarson, S. Guðmundsson, J. M. C. Belart, F. Pálsson, E. Magnússson, S. Víkingsson, I. Kaldal and T. Jóhannesson 2020. Variations in glacier extent in Iceland since the end of the Little Ice Age. *Jökull*, 70, 1–34. https://doi.org/10.33799/jokull2020.70.001

Hannesdóttir, H. 2020. Jöklabreytingar (Glacier variations) 1930–1970, 1970–1995, 1995–2018 og 2018–2019. *Jökull*, 70, 111–118. http://doi.org/110.33799/-jokull2020.70.111o

Hugonnet, R., R. McNabb, E. Berthier, B. Menounos, C. Nuth, L. Girod, D. Farinotti, M. Huss, I. Dussaillant, F. Brun and A. Kääb 2021. Accelerated global glacier mass loss in the early twenty-first century. *Nature* 592, 726–731. http://doi.org/10.1038/s41586-021-03436-z

Ives, J. D. and C. A. M. King 1954. Glaciological observations on Morsárjökull, SW Vatnajökull. Pt. I: The ogive banding. *J. Glaciol.* 2(16), 423–428. http://doi.-org/10.3189/002214354793702443

Ives, J. D. and C. A. M. King 1955. Glaciological observations on Morsárjökull, SW Vatnajökull. Pt. II: Regime of the glacier, present and past. *J. Glaciol.* 2(17), 477–482. http://doi.org/10.3189/002214355793702325

Jóhannesson, T., H. Björnsson, E. Magnússon, Sv. Guðmundsson, F. Pálsson, O. Sigurðsson, Th. Thorsteinsson and E. Berthier 2013. Ice-volume changes, bias estimation of mass-balance measurements and changes in subglacial lakes derived by lidar mapping of the surface of Icelandic glaciers. *Ann. Glaciol.* 54(63), 63–74. http://doi.org/10.3189/2013AoG63A42

Joughin, I. 2002. Ice-sheet velocity mapping: A combined interferometric and speckle-tracking approach. *Ann. Glaciol.*, 34, 195–201. http://doi.org/10.3189/-172756402781817978

Magnússon, E. 2008. *Glacier hydraulics explored by means of SAR-interferometry.* PhD thesis, University of Innsbruck.

Magnússon, E., H. Rott, H. Björnsson and F. Pálsson 2007. The impact of jökulhlaups on basal sliding observed by SAR interferometry on Vatnajökull, Iceland. *J. Glaciol.* 53(181), 232–240. http://doi.org/10.3189/-172756507782202810

Magnússon, E., H. Björnsson, H. Rott and F. Pálsson 2010. Reduced glacier sliding caused by persistent drainage from a subglacial lake. *Cryosph.* 4(1), 13–20. http://-doi.org/10.5194/tc-4-13-2010

Magnússon, E., H. Björnsson, H. Rott, M. J. Roberts, F. Pálsson, S. Guðmundsson, R. A. Bennett, H. Geirsson and E. Sturkell 2011. Localized uplift of Vatnajökull, Iceland: subglacial water accumulation deduced from InSAR and GPS observations. *J. Glaciol.*, 57(203), 475–484. http://doi.org/10.3189/-002214311796905703

Minchew, B. M., M. Simons, S. Hensley, H. Björnsson and F. Pálsson 2015. Early melt-season velocity fields of Langjökull and Hofsjökull ice caps, central Iceland.

J. Glaciol., 61(226), 253–266. http://doi.org/10.3189/-2015JoG14J023

Minchew, B. M., M. Simons, H. Björnsson, F. Pálsson, M. Morlighem, H. Seroussi, E. Larour and S. Hensley 2016. Plastic bed beneath Hofsjökull Ice Cap, central Iceland, and the sensitivity of ice flow to surface meltwater flux. *J. Glaciol.* 62(231), 147–158. http://-doi.org/10.1017/jog.2016.26

Mouginot, J., E. Rignot, B. Scheuchl and R. Millan 2017. Comprehensive Annual Ice Sheet Velocity Mapping Using Landsat-8, Sentinel-1, and RADARSAT-2 Data. *Remote Sens.* 9(4), 364. http://doi.org/10.3390/-rs9040364

Mouginot, J., E. Rignot, A. A. Bjørka, M. van den Broeke, R. Millan, M. Morlighem, B. Noël, B. Scheuchl and M. Wood 2018. Forty-six years of Greenland Ice Sheet mass balance from 1972 to 2018. *Proc. Natl. Acad. Sci.* 116(10), 9239–9244. http://doi.org/-10.1073/pnas.1904242116

Mouginot, J., E. Rignot and B. Scheuchl 2019. Continent-wide, interferometricSAR phase, mapping of Antarctic ice velocity. *Geophys. Res. Lett.*, 46, 9710–9718. http://doi.org/10.1029/2019GL083826

Morlighem, M., E. Rignot, H. Seroussi, E. Larour, H. Ben Dhia and D. Aubry 2010. Spatial patterns of basal drag inferred using control methods from a full-stokes and simpler models for Pine Island glacier, West Antarctica. *Geophys. Res. Lett.* 37(14), 114502. http://doi.-org/10.1029/2010GL043853

Nagler, T., H. Rott, M. Hetzenecker, K. Scharrer, E. Magnússon, D. Floricioiu and C. Notarnicola 2012. Retrieval of 3D-glacier movement by high resolution X-band SAR data. In Proceedings of the 2012 IEEE International Geoscience and Remote Sensing Symposium, Munich, Germany, 22–27 July 2012; 3233–3236. http://doi.org/10.1109/IGARSS.2012.6350735

Nagler, T., H. Rott, M. Hetzenecker, J. Wuite and P. Potin 2015. The Sentinel-1 mission: New opportunities for ice sheet observations. *Remote Sens.* 7, 9371–9389. http://doi.org/10.3390/rs70709371

Nagler, T., H. Rott, E. Ripper, G. Bippus and M. Hetzenecker 2016. Advancements for snowmelt monitoring by means of Sentinel-1 SAR. *Remote Sens.* 8(4), 348. http://doi.org/10.3390/rs804034

Pálsson, S. 2004 (written 1795). *Draft of a Physical, Geographical, and Historical Description of Icelandic Ice Mountains of the Basis of a Journey to the Most Prominent of Them in 1792–1794. An annotated and illustrated English translation* Williams, Jr., R. S. and O. Sigurðsson (eds.), Reykjavík, The Icelandic Literary Society.

Raymond, C. F. 1997. How do glaciers surge? *Geophys. Res.: Solid Earth* 92(B9), 9121–9134. http://-doi.org/10.1029/JB092iB09p09121

Rignot, E., D. Vaughan, M. Schmeltz, T. Dupont and D. MacAyeal 2002. Acceleration of Pine Island and Thwaites glaciers, West Antarctica. *Ann. Glaciol.* 34, 189–194.

Rignot, E., J. Mouginot, B. Scheuchl, M. van den Broeke, M. J. van Wessem and M. Morlighem 2019. Four decades of Antarctic Ice Sheet mass balance from 1979–2017. *Proc. Natl. Acad. Sci.* 116(4), 1095–1103. http://doi.org/10.1073/pnas.1812883116.

Sigurðsson, O., R. S. Williams and S. Víkingsson 2017. *Jöklakort af Íslandi, 2. útgáfa [Map of the Glaciers of Iceland, 2nd ed.].* Reykjavík, Icel. Meteorol. Office.

Strozzi, T., A. Luckman, T. Murray, U. Wegmuller and C. L. Werner 2002. Glacier motion estimation using SAR offset-tracking procedures. *IEEE Trans. Geosc. Rem. Sens.* 40(11), 2384–2391. http://doi.org/-10.1109/TGRS.2002.805079

Strozzi, R., F. Paul, A. Wiesmann, T. Schellenberger and A. Kääb 2017. Circum-Arctic changes in the flow of glaciers and ice caps from satellite SAR data between the 1990s and 2017. *Remote Sens.* 9(9), 947. http://-doi.org/10.3390/rs9090947

Torell, O. 1857. Bref om Island. Öfversigt af Kongl. Vetenskaps Akademiens Förhandl. 1857, nr. 9. Stockholm.

Wuite, J., L. Libert, T. Nagler and T. Jóhannesson 2021. Ice-velocity data set accompanying the paper: "Continuous monitoring of ice dynamics in Iceland with Sentinel-1". https://doi.org/10.5281/zenodo.5517241

Yagüe-Martínez, N., P. Prats-Iraola, F. Rodríguez González, R. Brcic, R. Shau, D. Geudtner, M. Eineder and R. Bamler 2015. Interferometric Processing of Sentinel-1 TOPS Data. *IEEE Trans. Geosci. Rem. Sens.* 54(4), 2220–2234. http://doi.org/10.1109/-TGRS.2015.2497902

Þórarinsson, S. 1939. Vatnajökull. Scientific results of the Swedish–Icelandic investigations 1936–37–38. Chapter VIII. Hoffelsjökull, its movements and drainage. *Geogr. Ann.* 21(3–4), 189–215. http://doi.org/10.1080/20014422.1939.11880678